HHS Public Access

Author manuscript

*Gastroenterology*. Author manuscript; available in PMC 2020 December 01.

Published in final edited form as:

*Gastroenterology*. 2019 December ; 157(6): 1572–1583.e8. doi:10.1053/j.gastro.2019.08.025.

# Interleukin 1 beta and Matrix Metallopeptidase 3 Contribute to Development of EGFR-dependent Serrated Polyps in Mouse Cecum

**Zhengxiang He**[1,*], **Lili Chen**[1,*], **Grace Chen**[1,*], **Paola Smaldini**[1], **Gerold Bongers**[2], **Jovani Catalan-Dibene**[1], **Glaucia C. Furtado**[1], **Sergio A. Lira**[1]

[1]Precision Immunology Institute, Icahn School of Medicine at Mount Sinai, New York, New York, USA

[2]Department of Oncological Sciences, Icahn School of Medicine at Mount Sinai, New York, New York, USA

## Abstract

**Background & Aims:** Transgenic mice (*HBUS*) that express the epidermal growth factor (EGFR) ligand HBEGF and a constitutively active G protein-coupled receptor (US28) in intestinal epithelial cells develop serrated polyps in the cecum. Development of serrated polyps depends on the composition of the gut microbiota and is associated with bacterial invasion of the lamina propria, accompanied by induction of inflammation and upregulation of interleukin 1 beta (IL1B) and matrix metalloproteinase 3 (MMP3) in the cecum. We investigated the mechanisms by which these changes contribute to development of serrated polyps.

**Methods:** We performed studies with C57BL/6 (control) and *HBUS* mice. To accelerate polyp development, we increased the exposure of the bacteria to the lamina propria by injecting *HBUS* mice with diphtheria toxin, which binds transgenic HBEGF expressed by the epithelial cells and causes apoptosis. Mice were given injections of IL1B-neutralizing antibody and the MMP inhibitor NNGH. Intestinal tissues were collected from mice and analyzed by histology, reverse-transcription PCR, ELISAs, immunofluorescence, and flow cytometry. We examined fibroblast subsets in polyps using single-cell RNA sequencing.

**Results:** Administration of diphtheria toxin to *HBUS* mice accelerated development of serrated polyps (95% of treated mice developed polyps before 100 days of age, compared to 53% given

**Correspondence:** Sergio A. Lira, M.D. Ph.D., Precision Immunology Institute, Icahn School of Medicine at Mount Sinai, 1425 Madison Ave. Box 1630 Room 12-20, New York, NY 10029, Phone (212) 659-9404; FAX (212) 849-2525, sergio.lira@mssm.edu.

*Authors share co-first authorship

Author Contributions:

Z.H., L.C. and G.C. designed study, did experiments, analyzed data, wrote and reviewed the manuscript. P.S., G.B., J.C-D. and G.C.F. did experiments, analyzed data and reviewed the manuscript. S.A.L. designed study, analyzed data, wrote and reviewed the manuscript.



Conflicts of Interest:

The authors disclose no conflicts of interests.

vehicle). IL1B stimulated subsets of platelet derived growth factor receptor alpha (PDGFRA)-positive fibroblasts isolated from cecum, resulting in increased expression of MMP3. Neutralizing antibodies against IL1B or administration of the MMP inhibitor reduced the number of serrated polyps that formed in the *HBUS* mice. Single-cell RNA sequencing analysis revealed subsets of fibroblasts in serrated polyps that express genes that regulate matrix fibroblasts and inflammation.

**Conclusions:** In studies of mice, we found that barrier breakdown and expression of inflammatory factors contribute to development of serrated polyps. Subsets of cecal PDGFRA-positive fibroblasts are activated by release of IL1B from myeloid cells during early stages of serrated polyp development. MMP3 produced by PDGFRA-positive fibroblasts is important for serrated polyp development. Our findings confirm the functions of previously identified serrated polyp-associated molecules, and indicate roles for immune and stromal cells in serrated polyp development.

## Graphical Abstract

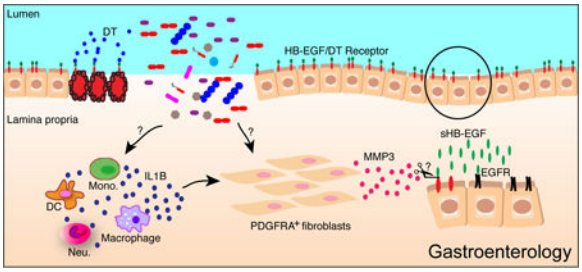


## Lay Summary

We studied mice that develop serrated polyps, and identified cells and proteins that contribute to their development. Strategies to block these cells or proteins might be developed for prevention of colon polyps.

### Keywords

neoplasm; cytokine; stroma; barrier breakdown

## Introduction

The two major groups of colorectal epithelial polyps are adenomas and serrated polyps (SPs). SPs are a heterogeneous group of lesions with variable malignant potential. They can be subdivided into hyperplastic polyps, traditional serrated adenomas/polyps, and sessile serrated polyps [1]. Small hyperplastic polyps were viewed as innocuous lesions with no potential for progression to malignancy [2]. However, published reports have demonstrated an association between colorectal adenocarcinomas and giant hyperplastic polyps (usually defined as >1 cm), suggesting that at least some hyperplastic polyps may have malignant potential [3, 4]. In addition, a condition known as hyperplastic polyposis syndrome characterized by the presence of multiple serrated lesions (either hyperplastic polyps or sessile serrated adenomas) throughout the colon is associated with an increased risk of developing colorectal cancer [5].

Activating mutations in components of the mitogen-activated protein kinase (MAPK) pathway have been associated with serrated lesions. One of the upstream components of the MAPK signaling pathway is the epidermal growth factor receptor (EGFR). The expression of EGFR and its ligands is often higher in gastrointestinal tumors than in surrounding normal tissue[6]. In addition, our previous studies have shown that EGFR activation is associated with SPs in human biopsies and that expression of the EGFR ligand heparin-binding epidermal growth factor-like growth factor (HBEGF) by intestinal epithelial cells of transgenic mice (*HBGF* mice) promotes development of SPs that mostly resemble human hyperplastic polyps [7]. Development of serrated polyps occurs, however, in only 5% of the *HBGF* transgenic mice. The incidence of serrated polyps is markedly increased by intercrossing *HBGF* mice with mice expressing US28 is a constitutively active chemokine receptor in intestinal epithelial cells. US28 is encoded by human herpesvirus 5, a highly prevalent human virus that infects a broad spectrum of cells, including intestinal epithelial cells [8]. US28 increases the cleavage of membrane bound HBEGF, to exacerbate development of SPs induced by HBEGF[7]. EGFR signaling is essential for development of SPs since its pharmacological inhibition prevents SP formation in *HBUS* mice[7]. However, the combined activity of HBEGF and US28 is not sufficient to drive polyp development because germ-free *HBUS* mice do not develop polyps. SP development in *HBUS* mice depends on the presence of a host-specific microbiota and is associated with bacterial invasion of the lamina propria accompanied by marked inflammatory changes in SPs [10].

The presence of bacteria in the lamina propria of SPs triggers an inflammatory response that includes upregulation of several cytokines, chemokines, and an HBEGF-processing metalloproteinase, matrix metalloproteinase (MMP)3 [10]. Among the cytokines interleukin 1 beta (IL1B) is a major mediator of inflammation[11]. IL1B has been shown to be an important inflammatory factor contributing to tumor development[12]. Of note, IL1B expression is upregulated in the SPs in both human [13]and mouse[10]. It is well known that cytokines stimulate production of MMPs through the activation of cellular signaling pathways involving MAPKs[14, 15]. We hypothesized that pro-inflammatory cytokine IL1B could act on stromal cells to induce expression of MMP3, increase membrane bound HBEGF cleavage and promote SPs development. In this study, we explored the functional relevance of these molecules (IL1B and MMP3) for the development of SPs. To increase the likelihood of intestinal barrier disruption we took advantage of the fact that member-bound HBEGF serves as a receptor for diphtheria toxin (DT)[16], and that its ligation promotes epithelial apoptosis. Treatment of *HBUS* mice with DT promoted apoptosis of intestinal epithelial cells, increased barrier permeability and accelerated polyp development. Using this protocol, we observed increased expression of IL1B by infiltrating and resident myeloid cells and increased expression of MMP3 by platelet-derived growth factor receptor alpha (PDGFRA) $^{+}$ fibroblasts. Inhibition of MMP activities reduced SP incidence, suggesting a critical role for MMPs in the development of SP. Together, these results confirm an important role for barrier breakdown in serrated polyp development, confirm functional roles for the previously identified SP-associated molecules, and suggest important role for immune and stromal cells in serrated polyp development.

## Methods

### Mice

*US28, HBGF* and *HBUS* mice were previously described [7, 9, 10]. No statistical method was used to determine sample size, and when applicable, mice were assigned to a treatment group using a simple randomization (coin flip). Mice were maintained under specific pathogen-free (SPF) conditions at the Icahn School of Medicine at Mount Sinai. *HBUS* and C57BL/6 wild-type Germ-free (GF) mice were housed in standard flexible film isolators. All animal experiments in this study were approved by the Institutional Animal Care and Use Committee of Icahn School of Medicine at Mount Sinai and were performed in accordance with the approved guidelines for animal experimentation at the Icahn School of Medicine at Mount Sinai.

### Diphtheria toxin (DT) treatment

Mice were intraperitoneally (i.p.) injected with DT. The experimental scheme is shown in Figure 1A. Briefly, each mouse received three doses of DT, once per week with increasing doses (week 1: 0.2ng/g, week 2: 0.25ng/g and week 3: 0.3ng/g), and was sacrificed three weeks after the last DT injection.

### EGFR inhibitor treatment

The EGFR inhibitor gefitinib (75 mg/kg, Sigma-Aldrich, St Louis, MO) were dissolved in 0.2% (vol/wt) Tween-80 (Sigma-Aldrich, St Louis, MO) and administered daily by oral gavage [7] for 35 days.

### *In vivo* cytokine neutralization

For neutralization of IL1B, anti-IL1B mAb clone B122 (Bio X Cell) was injected at 50 μg i.p. twice every week for the duration of the experiment (35 days).

### *In vivo* MMP inhibition

For MMP inhibition, MMP inhibitor, NNGH (N-Isobutyl-N-(4-methoxyphenylsulfonyl)glycyl Hydroxamic acid) (Cayman chemical) was injected at 160 μg dissolved in 3% DMSO i.p. three times per week for the duration of the experiment (35 days). The vehicle (3% DMSO) injections with *HBUS* mice were used as vehicle control group.

### RNA extraction and RT-qPCR

RNA extraction and reverse-transcription polymerase chain reaction (RT-qPCR) experiments were performed as previously described[17].

### IL1B enzyme-linked immunosorbent assay

Tissue homogenates were performed as previously described[7]. IL1B was quantified in tissue homogenates prepared from SPs and unaffected surrounding cecal tissues by enzyme-linked immunosorbent assay (ELISA) according to standard manufacturer's recommendations (R&D systems).

### Histology and Immunofluorescence staining

Histological analyses, immunofluorescence staining and fluorescent imaging were performed as previously described[10]. Primary antibodies were obtained from Cell signaling (cleaved caspase-3 and phospho-ERK1/2), Abcam (pan-keratin, IL1B, vimentin, and MMP3), R&D Systems (PDGFRA), or eBioscience (CD45).

### Flow cytometry analyses of cecal tissue

Flow cytometry analyses of cecal tissue were performed as previously described[10]. See Supplementary Material for details.

### Single-cell RNA sequencing for stromal cells

The flow-sorted cellular suspensions ($DAPI^{-}CD45^{-}CD31^{-}Epcam^{-}$) were loaded on a 10x Genomics platform for single-cell RNA-Sequencing analysis. See Supplementary Material for details.

### Mouse transcriptome analysis

RNA-Seq data from GF and SPF *HBUS* and C57BL/6 wild-type (WT) tissue samples were analyzed as described before[10].

### Statistical Analysis

Except for deep-sequencing data, statistical analyses were performed with GraphPad Prism 7 software (GraphPad, La Jolla, CA). Differences between groups were analyzed with nonparametric Mann–Whitney test or Fisher's exact test. Differences were considered significant when $P < .05$ and levels of significance are specified throughout the figure legends. Data are shown as mean values ± standard error of the mean (SEM) throughout.

## Results

### Diphtheria toxin (DT) administration accelerates polyp formation in *HBUS* mice

Previously, our laboratory has shown that *HBUS* mice, which express an EGFR ligand (HBEGF) and a constitutively active G-protein-coupled receptor (US28) in the intestinal epithelium, develop cecal serrated polyps (SPs).[7]. Microbiota contribute to the development of SPs since alterations of the microbiota induced by antibiotic treatment or by embryo transfer rederivation attenuate the formation of cecal SPs in *HBUS* mice [10]. SP development is associated with bacterial invasion of the lamina propria, which elicit local inflammatory responses [10]. We hypothesized that exacerbated inflammatory responses within the lamina propria in response to increased epithelial cell death and excessive exposure to microbial antigens from compromised epithelial barrier would affect SP development in *HBUS* mice. To induce epithelial cell death we treated *HBUS* mice with diphtheria toxin (DT) since the membrane anchored form of HBEGF functions as the DT receptor [18]. Internalization of bound DT inhibits protein synthesis and triggers apoptotic death of epithelial cells that express HBEGF [19, 20]. DT treatment of *HBUS* mice increased the number of apoptotic epithelial cells in the cecum (cleaved Caspase $3^{+}$ cells) (Supplementary Figure 1). To examine whether increased apoptosis of epithelial cells had functional consequences, we

treated ceca obtained from *HBUS* mice with sulfo-NHS-biotin. Sulfo-NHS-biotin can be used to examine permeability of tight junction proteins ex vivo[10]. Sulfo-NHS-biotin is a membrane- and tight junction–impermeable molecule that efficiently biotinylates primary amine-containing macromolecules such as proteins. We examined the biotin signal at the intestinal epithelium of *HBUS* mice before DT injection. The intestine was uniformly labeled, with no dye being detected in the lamina propria before DT injection (Supplementary Figure 2). In DT-treated *HBUS* mice the biotin signal could be clearly detected in the lamina propria (Supplementary Figure 2). These results indicate that DT treatment promoted epithelial cell apoptosis and suggest that the increased apoptosis led to increased epithelial permeability.

Next we tested whether DT administration could accelerate development of SPs in the *HBUS* mice. We intraperitoneally (i.p.) injected 3 doses of DT, once per week, with increasing doses (week 1: 0.2ng/g; week 2: 0.25ng/g; week 3: 0.3ng/g) and sacrificed the mice 3 weeks after the last DT administration (Figure 1A). We started the DT administration as early as 34 days of age and all mice were sacrificed by 100 days of age. This treatment led to development of SPs in 95% of mice within 5 weeks after DT treatment (Figure 1B and C). The polyps in treated mice were found exclusively in the cecum, were protuberant and well-circumscribed, and had an average size of approximately 10 $mm^2$. Microscopically, they were similar to SPs developed by *HBUS* mice without DT treatment [7] (Figure 1D). Of note, the percentage of *HBUS* mice that developed SP before 100 days of age increased from 53% to 95% as the result of DT administration (Figure 1E). These results indicate that DT treatment accelerated polyp development in *HBUS* mice.

EGFR signaling is known to activate the MAPK pathway, leading to increased phosphorylation of ERK1/2 [7]. To investigate if DT administration would affect HBEGF-EGFR signaling we performed immunostaining of phospho-ERK1/2 (P-ERK1/2). We found that P-ERK1/2 phosphorylation was increased in the polyps of *HBUS* mice injected with DT (Supplementary Figure 3A), similar to what had been observed in *HBUS* mice. To further confirm the importance of EGFR signaling in DT-treated *HBUS* mice we used the EGFR inhibitor gefitinib (Supplementary Figure 3B). We found that gefitinib treatment markedly reduced the incidence of polyps (Supplementary Figure 3C). These results indicate that that EGFR activation by HBEGF is the dominant factor for development of polyps in *HBUS* mice after administration of DT. The microbiota is required for development of polyps in *HBUS* mice, as documented by treatment with large spectrum antibiotics or studies in germ-free conditions (Supplementary Figure 5A). To address if the intestinal microbiota played a role in SP development in DT-treated *HBUS* mice, we treated *HBUS* mice with DT and a broad-spectrum antibiotic cocktail (metronidazole, ampicillin, neomycin, and vancomycin) and examined the SP incidence after 35 days (Supplementary Figure 4A). Treatment with antibiotics completely blocked polyp development in the DT-treated *HBUS* mice (Supplementary Figure 4B).

In summary, our results indicate DT administration increases apoptosis of epithelial cells, dysregulates intestinal permeability, and accelerates polyp formation in *HBUS* mice, and that this process is dependent on EGFR signaling and on the intestinal microbiota.

### Increased expression of proinflammatory cytokine, IL1B, in SPs of *HBUS* mice

Our previous studies show that the proinflammatory cytokine genes *Il1a, Il1b*, and *Tnf* are significantly upregulated in murine SPs compared with unaffected surrounding cecal tissues [10]. Of note, IL1B expression is also found to be upregulated in human SPs [13]. To confirm that IL1B gene expression was also significantly upregulated in SPs of DT-treated *HBUS* mice we performed experiments described in Figure 2. IL1B expression was increased in SP compared to surrounding tissue at the mRNA (Figure 2A) and protein level (Figure 2B). In agreement with these findings, immunofluorescence staining of cecal sections of DT-treated *HBUS* mice with an antibody against IL1B revealed a higher number of $IL1B^+$ cells in SPs than in unaffected surrounding cecal tissue (Figure 2C). Interestingly, $IL1B^+$ cells were found in areas where the invasive bacteria were found previously [10], suggesting that these cells might be stimulated by bacterial antigens to produce IL1B. This hypothesis was supported by the observation that the expression of IL1B was comparable between GF *HBUS* mice and GF wildtype C57BL/6 mice (Supplementary Figure 5B), indicating that microbiota contributed to IL1B upregulation. We can not rule out that other factors, such as increased epithelial cell death or apoptotic cell debris in the lamina propria secondary to DT administration could elicit inflammatory responses and stimulate the production of proinflammatory mediators such as IL1B [21, 22]. Together, our results indicate an upregulation of IL1B in SPs and suggest that IL1B can be an important inflammatory mediator that promotes development of SPs.

### Myeloid populations are the primary source of IL1B in SPs

Next we tested which cell population produced IL1B in SPs. Flow cytometry analyses further confirmed that the number of $IL1B^+$ cells in SPs was higher than that of unaffected surrounding cecal tissue (Figure 3A and B). The majority of $IL1B^+$ cells were $CD45^+CD11b^+$ cells both in SPs and in surrounding tissues (Figure 3A and Supplementary Figure 6), which is consistent with literature that IL1B is produced by $CD45^+$ hematopoietic cells such as blood monocytes, tissue macrophages, and dendritic cells in response to toll-like receptor ligands, other cytokines and complement components [23]. Epithelial cells ($Epcam^+$) did not produce IL1B (Supplementary Figure 6). Indeed, almost all the myeloid populations including resident macrophage, dendritic cell (DC), inflammatory macrophages/monocytes and neutrophils, could produce IL1B (Supplementary Figure 6). However, compared to the unaffected surrounding cecal tissue, the proportion of inflammatory macrophages/monocytes and neutrophils producing IL1B was significantly increased in SPs (Figure 3C). In addition, compared to other IL1B producing myeloid cells in SP, inflammatory macrophages/monocytes cells produced significantly higher amount of IL1B (Figure 3D). Our data thus suggest that myeloid populations are the source of IL1B in SPs and that IL1B is predominantly produced by inflammatory macrophages/monocytes.

### IL1B neutralization reduces SP incidence in *HBUS* mice

To determine whether IL1B plays a role in the pathology of SPs, we subjected DT-treated *HBUS* mice to anti-IL1B (clone B122) treatment and examined the SP incidence and size after 35 days (Figure 4A). Treatment with anti-IL1B antibody led to a 50% reduction in SP incidence. Whereas 80% of isotype-treated mice developed SPs, only 40% of anti-IL1B-

treated mice developed SPs (Figure 4B). However, the size of the SPs that developed in anti-IL1B-treated mice was not significantly reduced when compared to those of isotype-treated mice (Figure 4C). These results suggest that IL1B is important for the development of SP.

### PDGFRA$^+$ fibroblasts produce MMP3 *in vivo* and *in vitro* following IL1B stimulation

IL1B is a central mediator of inflammation and can activate a variety of cells [24] including fibroblasts [25]. To identify target cells of IL1B in SPs, we examined cells located at areas close to the lumen where clusters of IL1B$^+$ cells were found. Cells expressing platelet-derived growth factor receptor alpha (PDGFRA$^+$) were found in the lamina propria of SPs and were increased in the polyp compared to surrounding tissue (Supplementary Figure 7A). PDGFRA has been shown to be a marker for a subpopulation of fibroblasts in both mouse and human colon located just beneath the colonic epithelium and form pericryptal sheaths from the base to the top of crypts [26, 27]. In addition, PDGFRA is broadly expressed in neoplastic skin fibroblasts [28]. In SPs, PDGFRA$^+$ cells were CD45 negative (Supplementary Figure 7B) and vimentin positive (Supplementary Figure 7B), suggesting that these cells were fibroblasts.

Cytokines such as IL1B, IL17 and TNFA have been shown to induce MMP3 secretion in human myofibroblast [29]. Previously, we have demonstrated that both mRNA and protein expression of MMP3 are elevated in SPs of *HBUS* mice [10] which could mediate ectodomain shedding of HBEGF and thereby promote autocrine/paracrine EGFR signaling [30] and SP development. In our current DT paradigm, MMP3 mRNA (Figure 5A) and protein (Figure 5B) expression were similarly upregulated in SPs compared to unaffected surrounding tissues. Similar distribution of MMP3$^+$ and PDGFRA$^+$ cells in SPs suggested that PDGFRA$^+$ fibroblasts could be the MMP3-producing cells. We tested this hypothesis by performing double staining in tissue sections of SPs with antibodies against MMP3 and PDGFRA. Indeed, we found that PDGFRA$^+$ fibroblasts produced MMP3 in the SPs (Figure 5C). Co-localization of MMP3 and PDGFRA suggested that PDGFRA$^+$ fibroblasts in SPs produced MMP3 and could be a source of increased MMP3 in SPs.

To investigate whether PDGFRA$^+$ fibroblasts could produce MMP3 in response to IL1B, we sorted PDGFRA$^+$ fibroblasts from wildtype C57BL/6 mice and measured MMP3 mRNA and protein expression following IL1B stimulation. We observed a significant increase in mRNA expression of MMP3 in PDGFRA$^+$ fibroblasts in response to IL1B stimulation (Figure 5D). In addition, we quantified MMP3$^+$PDGFRA$^+$ fibroblasts by staining the cells with an anti-MMP3 antibody and DAPI following IL1B stimulation. Approximately 35% of cultured PDGFRA$^+$ fibroblasts produced MMP3 protein in response to IL1B (Figure 5E).

Similar to IL1B, expression of MMP3 was specifically upregulated in SPs but not in unaffected surrounding tissue (Figure 5B) or wildtype C57BL/6 cecum (Supplementary Figure 8). In addition, MMP3 expression was comparable between cecum from GF *HBUS* and GF C57BL/6 mice (Supplementary Figure 8), suggesting that the microbiota has a direct role in the induction of MMP3 expression. Our results thus suggest that upregulation of MMP3 in PDGFRA$^+$ fibroblasts in SPs requires an intact microbiota and IL1B signaling.

### Treating *HBUS* mice with the MMP inhibitor NNGH reduces SP incidence

To investigate whether increased expression of the HBEGF-processing metalloproteinase, MMP3, would promote SP development, we treated *HBUS* mice with a MMP inhibitor, NNGH, and examined SP incidence and size. Remarkably, treating *HBUS* mice with NNGH for 35 days reduced SP incidence by more than 50% (Figure 6A and B) but did not significantly change the size of SPs that developed in NNGH-treated mice (Figure 6C). These results suggest that MMP activity is important for the development of SPs in *HBUS* mice.

### SPs contain distinct fibroblast populations

Our results suggest that fibroblasts contribute to SP development via expression of MMP3. Fibroblasts associated with the development of intestinal neoplasm are a complex and heterogeneous population of cells with diverse functions and molecular markers [31]. To analyze SP-associated fibroblasts in detail, we performed single-cell RNA sequencing (scRNA-seq) with mesenchymal preparations from SPs. We obtained enriched mesenchymal cells by fluorescence-activated cell sorting (FACS) $CD45^{-}CD31^{-}$ $EpCAM^{-}$ cells from SP homogenates and performed scRNA-seq using the 10x Genomics Chromium platform. We profiled 2053 cells from *HBUS* SPs and visualized the cells in two dimensions according to their expression profiles by t-distributed stochastic neighborhood embedding (t-SNE) projections. The number of contaminating $CD45^{+}$ (*ptprc)* hematopoietic cells, $CD31^{+}$ (*pecam1*) endothelial cells, and $EpCAM^{+}$ (*epcam*) epithelial cells was minimal. These cells were easily identified and eliminated from further analysis. Six clusters of fibroblasts in SPs were well segregated (Figure 7A). We classified these clusters based on their distinctive marker expression and relations to known cell types. Using known marker genes for pericytes such as *rgs5* and *pdgfrb*, a pericyte cluster in SPs was readily identified (Figure 7A and B). Interestingly, this population also expressed high levels of known myofibroblast markers, including *acta2* [32], *myl9* [33] and *tagln* [33, 34] (Figure 7A and B). We identified a small population of fibroblasts in SPs that expressed distinct markers of proliferative mesenchymal progenitors, including *hist1h2ap*, *cks2*, *hmgb2*, *ube2c*, *h2afx*, and *ccnb2,* which are associated with cell cycle and proliferation [33, 35]. The third cluster of fibroblasts was characterized by a signature enriched with genes involved in Wnt and Bmp pathways which are key signaling pathways supporting proliferation and differentiation of the intestinal stem cells [27], suggesting that this cluster represents subepithelial myofibroblasts in SPs (Figure 7A and B).

The remaining three cell clusters (stromal 1, 2 and 3) were characterized by genes that have been previously shown to associate with matrix fibroblasts such as *col14al*, *pi16*, *cd81*, *mfap5*, and *fbn1* [33, 35] (Figure 7A and B). In addition, stromal 1 and 2 showed higher expression of inflammatory chemokines *ccl7*, *ccl2*, *cxcl1*, and inflammatory mediator, *il6*, *klf4*, suggesting that these fibroblasts are proinflammatory (Figure 7A and B).

We examined how expression of *pdgfra* and *MMP3* segregated across mesenchymal subsets identified by scRNA-seq. *Pdgfra* expression was present in all subsets except for pericyte/myofibroblast subset whereas *MMP3* expression was found mostly in stromal 1, 2 and 3, the three populations characterized by low αSMA (*acta2*) expression (Figure 7C). Our data

suggest that subsets of fibroblasts in SPs characterized by the expression of both matrix fibroblast-associated genes and proinflammatory genes are the likely source of increased MMP3 in SPs.

## Discussion

We have previously shown that EGFR is activated in a subset of human SPs[7]. In a subsequent study we showed that animals carrying HBEGF, a membrane bound ligand for EGFR, develop serrated polyps in the cecum and that the microbiota is required for the development of these lesions[10]. In the present manuscript, we sought to define how these processes evolve mechanistically. We reasoned that epithelial lesions and bacteria would be critical for development of polyps, and that specific inflammatory factors could also contribute to polyp development. To test these hypotheses we took advantage of the fact that member-bound HBEGF also serves as a receptor of DT, and promote epithelial apoptosis. We show here that DT administration increases epithelial apoptosis in *HBUS* mice, and that this is associated with increased permeability. We also demonstrate a critical requirement for the microbiota for the development of polyps because treatment of mice with an antibiotic cocktail and DT inhibited polyp development. Importantly, DT injection in *HBUS* mice accelerated polyp development. Using this protocol, the percentage of *HBUS* mice that developed SP before 100 days of age increased from 53% to 95%. The high penetrance of the SP phenotype within a shorter period of time allowed us to perform mechanistic studies that reveal an important role for the inflammatory cytokine IL1B in SP development.

We show that IL1B is predominantly produced by myeloid population and that it stimulates the production of matrix-degrading enzyme, MMP3, from subsets of PDGFRA$^+$ fibroblasts characterized by upregulation of extracellular matrix (ECM)- and inflammation-related genes. We show a more than 50% reduction in SP incidence by inhibiting MMP activities with a cell-permeable, broad-spectrum inhibitor, demonstrating a critical role for MMPs in SP development. These findings provide evidence that inflammatory macrophages/monocytes and stromal fibroblasts work in concert to drive the development of SPs. The precise mechanism by which MMPs contribute to SP development is currently under investigation. One possibility is that MMPs mediate the proteolytic cleavage of membrane bound HBEGF to generate soluble HBEGF which stimulates EGFR-mediated epithelial cell proliferation and SP development.

It is widely accepted that stromal fibroblasts have a profound influence on the development and progression of carcinomas [36–38]. Cancer-associated fibroblasts (CAFs) are known to support different aspects of tumor initiation, growth and progression by secretion of paracrine growth factors, ECM components and proteolytic enzymes [39, 40]. CAF-derived proteolytic enzymes such as MMPs are involved in several different stages of cancer development from angiogenesis, cancer cell growth and survival [41] to cancer invasion and metastasis [42, 43]. MMPs can promote cancer cell proliferation by assisting the release of growth factors from ECM components [44, 45]. In addition, MMPs participate in the release of cell-membrane-bound precursor forms of many growth factors, including transforming growth factor-α [46] and HBEGF [30]. Accordingly, MMPs could contribute to hyperproliferation of intestinal epithelium and SP formation since inhibition of MMP

activities reduces the SP incidence. We propose that membrane bound HBEGF, one of the transgenes in *HBUS* mice, is cleaved by active MMP3 found upregulated only in SPs but not unaffected surrounding tissue. This process could result in an elevation of soluble HBEGF in situ, activation of EGFR on epithelium, and polyp development. Because NNGH is a broad inhibitor of MMP activity we can not rule out that MMPs other than MMP3, may also be involved in the process.

CAFs are often described as myofibroblasts, characterized by αSMA expression [47], [48]; however, increasing evidence demonstrate that fibroblasts in tumor tissues are composed of $\alpha SMA^+$ myofibroblastic cells intermixed with other fibroblasts that do not express αSMA [28, 49]. Similarly, the majority of SP-associated fibroblasts that produce MMP3 in our model had low expression of αSMA and expressed genes associated with matrix proteins and inflammation. Proinflammatory CAFs have been described in mouse model of skin dysplasia, mammary and pancreatic adenocarcinoma and in human skin and pancreatic tumors, implicating a general role for fibroblast-mediated inflammation in multiple cancers [28]. Interestingly, the proinflammatory gene signature identified in CAFs from skin dysplastic tissue was already induced in fibroblasts isolated from the earlier hyperplastic stage of tumor progression, suggesting a prominent role for fibroblasts in both initiating and driving tumor-promoting inflammation in skin carcinogenesis [28]. The serrated polyps described here mostly resemble hyperplastic polyps in humans[7]. Fibroblasts in these lesions appear to have pro-inflammatory properties similar to fibroblasts associated with skin carcinoma. However, both mouse and human hyperplastic polyps have negligible malignant potential, which suggests that the fibroblasts in these specific serrated polyps are not capable of driving cancer development.

A recent publication, using unbiased single-cell profiling of colonic mesenchymal cells from healthy and inflamed colonic tissue, demonstrates heterogeneity in both human and mouse colonic fibroblasts but also a significicant degree of fibroblastic cell plasticity in disease. In colitis, there is an expansion of subpopulation of fibroblasts that uniquely gained lymph node fibroblastic reticular cell (FRC)-like features [50]. Interestingly, while we identify similar subsets of fibroblasts in our single-cell profiling (namely, subepithelial myofibroblasts and pericytes/myofibroblasts) the SP-associated fibroblasts do not contain a cell population with FRC-like features. These results further emphasize the plasticity of fibroblasts and suggest that fibroblasts are capable of upregulating different sets of genes which function to promote disease progression differently.

In summary, we have demonstrated that subsets of cecal $PDGFRA^+$ fibroblasts are activated by IL1B released from inflammatory macrophages during early stage of SP development. Proinflammatory genes and MMP3 are upregulated in these activated fibroblasts that can promote inflammation and SP development by facilitating HBEGF/EGFR signaling. These results highlight the functional importance of fibroblasts during early development of intestinal neoplasms and suggest that therapeutic targeting of fibroblast regulatory or effector circuits could be of value in preventing development and progression of SPs.

## Supplementary Material

Refer to Web version on PubMed Central for supplementary material.

## Acknowledgments:

We thank Dr. Madhura Deshpande for early contribution to this project. We thank the germ-free animal facility of the Icahn School of Medicine at Mount Sinai for expert support. We also thank Mr. Alan J. Soto (Biorepository and Pathology CoRE) for technical support with histology.

Funding:

This work was supported by a grant from the National Institutes of Health (R01 CA161373) to Sergio A. Lira. Lili Chen was supported by a Career Development Award (634253) from the Crohn's & Colitis Foundation of America (CCFA).

## Abbreviation:

| | |
|---|---|
| **CAF** | cancer-associated fibroblasts |
| **DT** | diphtheria toxin |
| **ECM** | extracellular matrix |
| **EGFR** | epidermal growth factor receptor |
| **GF** | germ-free |
| **HBEGF** | heparin-binding epidermal growth factor-like growth factor |
| **IL** | Interleukin |
| **MMP** | matrix metalloproteinase |
| **NNGH** | N-Isobutyl-N-(4-methoxyphenylsulfonyl)glycyl Hydroxamic acid |
| **PDGFRA** | platelet-derived growth factor receptor alpha |
| **scRNA** | seq single-cell RNA sequencing |
| **SP** | serrated polyp |
| **SPF** | specific pathogen-free |
| **WT** | wild-type |

## References

1. Rex DK, Ahnen DJ, Baron JA, et al. Serrated lesions of the colorectum: review and recommendations from an expert panel. Am J Gastroenterol 2012;107:1315–29; quiz 1314, 1330. [PubMed: 22710576]
2. O'Connell BM, Crockett SD. The clinical impact of serrated colorectal polyps. Clin Epidemiol 2017;9:113–125. [PubMed: 28260946]
3. Azimuddin K, Stasik JJ, Khubchandani IT, et al. Hyperplastic polyps: "more than meets the eye"? Report of sixteen cases. Dis Colon Rectum 2000;43:1309–13. [PubMed: 11005503]

4. Warner AS, Glick ME, Fogt F. Multiple large hyperplastic polyps of the colon coincident with adenocarcinoma. Am J Gastroenterol 1994;89:123–5. [PubMed: 8273780]
5. Boparai KS, Mathus-Vliegen EM, Koornstra JJ, et al. Increased colorectal cancer risk during follow-up in patients with hyperplastic polyposis syndrome: a multicentre cohort study. Gut 2010;59:1094–100. [PubMed: 19710031]
6. Messa C, Russo F, Caruso MG, et al. EGF, TGF-alpha, and EGF-R in human colorectal adenocarcinoma. Acta Oncol 1998;37:285–9. [PubMed: 9677101]
7. Bongers G, Muniz LR, Pacer ME, et al. A role for the epidermal growth factor receptor signaling in development of intestinal serrated polyps in mice and humans. Gastroenterology 2012;143:730–740. [PubMed: 22643351]
8. Sinzger C, Grefte A, Plachter B, et al. Fibroblasts, epithelial cells, endothelial cells and smooth muscle cells are major targets of human cytomegalovirus infection in lung and gastrointestinal tissues. J Gen Virol 1995;76 (Pt 4):741–50. [PubMed: 9049319]
9. Bongers G, Maussang D, Muniz LR, et al. The cytomegalovirus-encoded chemokine receptor US28 promotes intestinal neoplasia in transgenic mice. J Clin Invest 2010;120:3969–78. [PubMed: 20978345]
10. Bongers G, Pacer ME, Geraldino TH, et al. Interplay of host microbiota, genetic perturbations, and inflammation promotes local development of intestinal neoplasms in mice. J Exp Med 2014;211:457–72. [PubMed: 24590763]
11. Voronov E, Apte RN. IL-1 in Colon Inflammation, Colon Carcinogenesis and Invasiveness of Colon Cancer. Cancer Microenviron 2015;8:187–200. [PubMed: 26686225]
12. Krelin Y, Voronov E, Dotan S, et al. Interleukin-1beta-driven inflammation promotes the development and invasiveness of chemical carcinogen-induced tumors. Cancer Res 2007;67:1062–71. [PubMed: 17283139]
13. Szylberg L, Janiczek M, Popiel A, et al. Expression of COX-2, IL-1beta, TNF-alpha and IL-4 in epithelium of serrated adenoma, adenoma and hyperplastic polyp. Arch Med Sci 2016;12:172–8. [PubMed: 26925134]
14. Kyriakis JM, Avruch J. Mammalian mitogen-activated protein kinase signal transduction pathways activated by stress and inflammation. Physiol Rev 2001;81:807–69. [PubMed: 11274345]
15. Noh EM, Kim JS, Hur H, et al. Cordycepin inhibits IL-1beta-induced MMP-1 and MMP-3 expression in rheumatoid arthritis synovial fibroblasts. Rheumatology (Oxford) 2009;48:45–8. [PubMed: 19056796]
16. Iwamoto R, Higashiyama S, Mitamura T, et al. Heparin-binding EGF-like growth factor, which acts as the diphtheria toxin receptor, forms a complex with membrane protein DRAP27/CD9, which up-regulates functional receptors and diphtheria toxin sensitivity. EMBO J 1994;13:2322–30. [PubMed: 8194524]
17. Chen L, He Z, Iuga AC, et al. Diet Modifies Colonic Microbiota and CD4(+) T-Cell Repertoire to Induce Flares of Colitis in Mice With Myeloid-Cell Expression of Interleukin 23. Gastroenterology 2018;155:1177–1191 e16. [PubMed: 29909020]
18. Naglich JG, Metherall JE, Russell DW, et al. Expression cloning of a diphtheria toxin receptor: identity with a heparin-binding EGF-like growth factor precursor. Cell 1992;69:1051–61. [PubMed: 1606612]
19. Mitamura T, Higashiyama S, Taniguchi N, et al. Diphtheria toxin binds to the epidermal growth factor (EGF)-like domain of human heparin-binding EGF-like growth factor/diphtheria toxin receptor and inhibits specifically its mitogenic activity. J Biol Chem 1995;270:1015–9. [PubMed: 7836353]
20. Cummings RJ, Barbet G, Bongers G, et al. Different tissue phagocytes sample apoptotic cells to direct distinct homeostasis programs. Nature 2016;539:565–569. [PubMed: 27828940]
21. Nunes T, Bernardazzi C, de Souza HS. Cell death and inflammatory bowel diseases: apoptosis, necrosis, and autophagy in the intestinal epithelium. Biomed Res Int 2014;2014:218493. [PubMed: 25126549]
22. Yang Y, Jiang G, Zhang P, et al. Programmed cell death and its role in inflammation. Mil Med Res 2015;2:12. [PubMed: 26045969]

23. Dinarello CA. Interleukin-1 in the pathogenesis and treatment of inflammatory diseases. Blood 2011;117:3720–32. [PubMed: 21304099]
24. Garlanda C, Dinarello CA, Mantovani A. The interleukin-1 family: back to the future. Immunity 2013;39:1003–18. [PubMed: 24332029]
25. Witowski J, Thiel A, Dechend R, et al. Synthesis of C-X-C and C-C chemokines by human peritoneal fibroblasts: induction by macrophage-derived cytokines. Am J Pathol 2001;158:1441–50. [PubMed: 11290562]
26. Kurahashi M, Nakano Y, Peri LE, et al. A novel population of subepithelial platelet-derived growth factor receptor alpha-positive cells in the mouse and human colon. Am J Physiol Gastrointest Liver Physiol 2013;304:G823–34. [PubMed: 23429582]
27. Shoshkes-Carmel M, Wang YJ, Wangensteen KJ, et al. Subepithelial telocytes are an important source of Wnts that supports intestinal crypts. Nature 2018;557:242–246. [PubMed: 29720649]
28. Erez N, Truitt M, Olson P, et al. Cancer-Associated Fibroblasts Are Activated in Incipient Neoplasia to Orchestrate Tumor-Promoting Inflammation in an NF-kappaB-Dependent Manner. Cancer Cell 2010;17:135–47. [PubMed: 20138012]
29. Bamba S, Andoh A, Yasui H, et al. Matrix metalloproteinase-3 secretion from human colonic subepithelial myofibroblasts: role of interleukin-17. J Gastroenterol 2003;38:548–54. [PubMed: 12825130]
30. Suzuki M, Raab G, Moses MA, et al. Matrix metalloproteinase-3 releases active heparin-binding EGF-like growth factor by cleavage at a specific juxtamembrane site. J Biol Chem 1997;272:31730–7. [PubMed: 9395517]
31. Koliaraki V, Pallangyo CK, Greten FR, et al. Mesenchymal Cells in Colon Cancer. Gastroenterology 2017;152:964–979. [PubMed: 28111227]
32. Hinz B, Phan SH, Thannickal VJ, et al. The myofibroblast: one function, multiple origins. Am J Pathol 2007;170:1807–16. [PubMed: 17525249]
33. Du Y, Guo M, Whitsett JA, et al. 'LungGENS': a web-based tool for mapping single-cell gene expression in the developing lung. Thorax 2015;70:1092–4. [PubMed: 26130332]
34. Robin YM, Penel N, Perot G, et al. Transgelin is a novel marker of smooth muscle differentiation that improves diagnostic accuracy of leiomyosarcomas: a comparative immunohistochemical reappraisal of myogenic markers in 900 soft tissue tumors. Mod Pathol 2013;26:502–10. [PubMed: 23174934]
35. Xie T, Wang Y, Deng N, et al. Single-Cell Deconvolution of Fibroblast Heterogeneity in Mouse Pulmonary Fibrosis. Cell Rep 2018;22:3625–3640. [PubMed: 29590628]
36. Bhowmick NA, Neilson EG, Moses HL. Stromal fibroblasts in cancer initiation and progression. Nature 2004;432:332–7. [PubMed: 15549095]
37. Tripathi M, Billet S, Bhowmick NA. Understanding the role of stromal fibroblasts in cancer progression. Cell Adh Migr 2012;6:231–5. [PubMed: 22568983]
38. Liao Z, Tan ZW, Zhu P, et al. Cancer-associated fibroblasts in tumor microenvironment - Accomplices in tumor malignancy. Cell Immunol 2018.
39. Pietras K, Ostman A. Hallmarks of cancer: interactions with the tumor stroma. Exp Cell Res 2010;316:1324–31. [PubMed: 20211171]
40. Kalluri R The biology and function of fibroblasts in cancer. Nat Rev Cancer 2016;16:582–98. [PubMed: 27550820]
41. Egeblad M, Werb Z. New functions for the matrix metalloproteinases in cancer progression. Nat Rev Cancer 2002;2:161–74. [PubMed: 11990853]
42. Koshikawa N, Giannelli G, Cirulli V, et al. Role of cell surface metalloprotease MT1-MMP in epithelial cell migration over laminin-5. J Cell Biol 2000;148:615–24. [PubMed: 10662785]
43. Kim J, Yu W, Kovalski K, et al. Requirement for specific proteases in cancer cell intravasation as revealed by a novel semiquantitative PCR-based assay. Cell 1998;94:353–62. [PubMed: 9708737]
44. Manes S, Llorente M, Lacalle RA, et al. The matrix metalloproteinase-9 regulates the insulin-like growth factor-triggered autocrine response in DU-145 carcinoma cells. J Biol Chem 1999;274:6935–45. [PubMed: 10066747]

45. Whitelock JM, Murdoch AD, Iozzo RV, et al. The degradation of human endothelial cell-derived perlecan and release of bound basic fibroblast growth factor by stromelysin, collagenase, plasmin, and heparanases. J Biol Chem 1996;271:10079–86. [PubMed: 8626565]

46. Peschon JJ, Slack JL, Reddy P, et al. An essential role for ectodomain shedding in mammalian development. Science 1998;282:1281–4. [PubMed: 9812885]

47. Desmouliere A, Guyot C, Gabbiani G. The stroma reaction myofibroblast: a key player in the control of tumor cell behavior. Int J Dev Biol 2004;48:509–17. [PubMed: 15349825]

48. Micke P, Ostman A. Tumour-stroma interaction: cancer-associated fibroblasts as novel targets in anti-cancer therapy? Lung Cancer 2004;45 Suppl 2:S163–75. [PubMed: 15552797]

49. Sugimoto H, Mundel TM, Kieran MW, et al. Identification of fibroblast heterogeneity in the tumor microenvironment. Cancer Biol Ther 2006;5:1640–6. [PubMed: 17106243]

50. Kinchen J, Chen HH, Parikh K, et al. Structural Remodeling of the Human Colonic Mesenchyme in Inflammatory Bowel Disease. Cell 2018;175:372–386 e17. [PubMed: 30270042]

**BACKGROUND AND CONTEXT**

We performed studies with transgenic mice that develop serrated polyps in the cecum and investigated the mechanisms of polyp development.

**NEW FINDINGS**

Administration of diphtheria toxin to the transgenic mice accelerated development of serrated polyps. Cecal fibroblasts are activated by release of interleukin 1 beta from myeloid cells during early stages of serrated polyp development. A matrix metalloproteinase produced by these fibroblasts was required for serrated polyp development.

**LIMITATIONS**

This study was performed in a mouse model of serrated polyp development.

**IMPACT**

Barrier breakdown appears to contribute to development of serrated polyps. We identified immune and stromal cells that contribute to serrated polyp development.

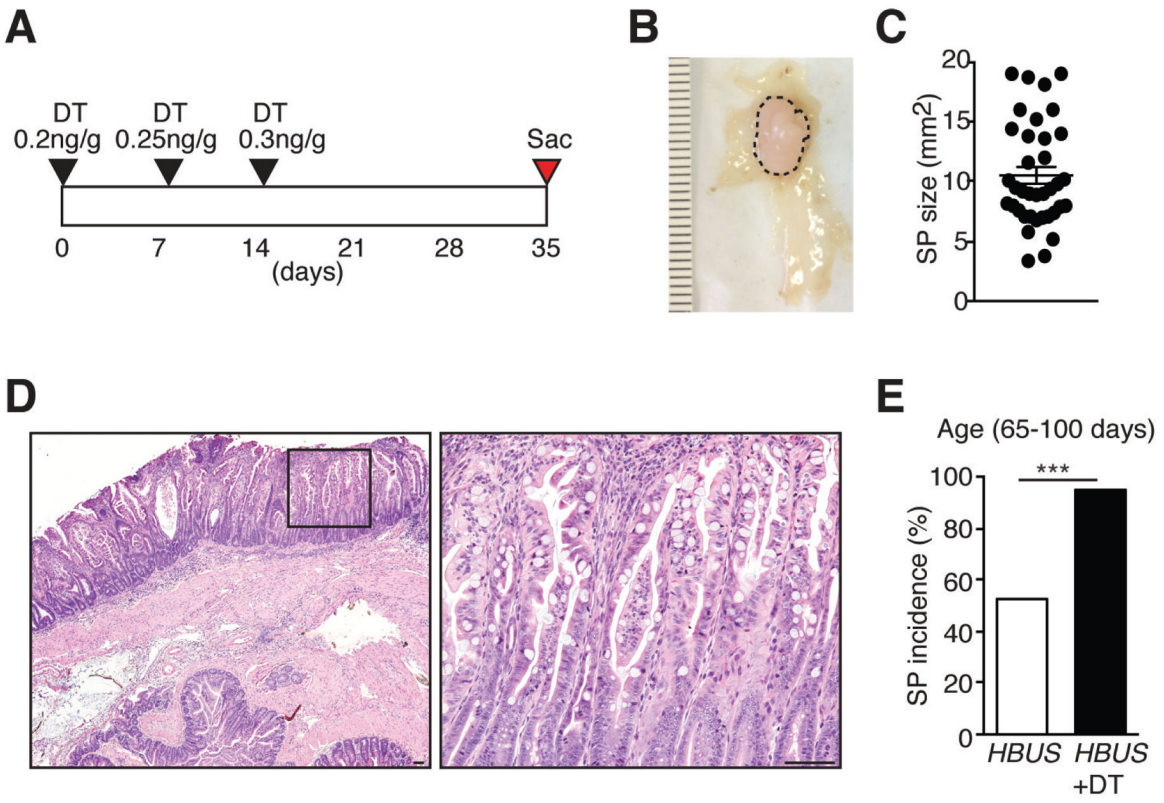


**Figure 1. Diphtheria toxin administration promotes serrated polyp formation in *HBUS* mice.**

(*A*) Schematic representation of diphtheria toxin (DT) administration. (*B*) Gross picture of the cecum of DT-treated *HBUS* mice on day 35 after first DT administration showing a serrated polyp (SP) (dashed lines). (*C*) Size of SP (n=37). Error bar indicates SEM. (*D*) Representative histological section of the cecum of DT-treated *HBUS* mice on day 35 after first DT administration. Inset (right panel) shows a higher-magnification image of left panel. Scale bars, 50 μm. (*E*) SP incidence in *HBUS* mice at age between 65–100 days old without DT injection (53%, n=38, white bar) compared with *HBUS* mice treated with DT at age between 65–100 days old (95%, n=39, black bar). ***$P < .001$, by Fisher's exact test.

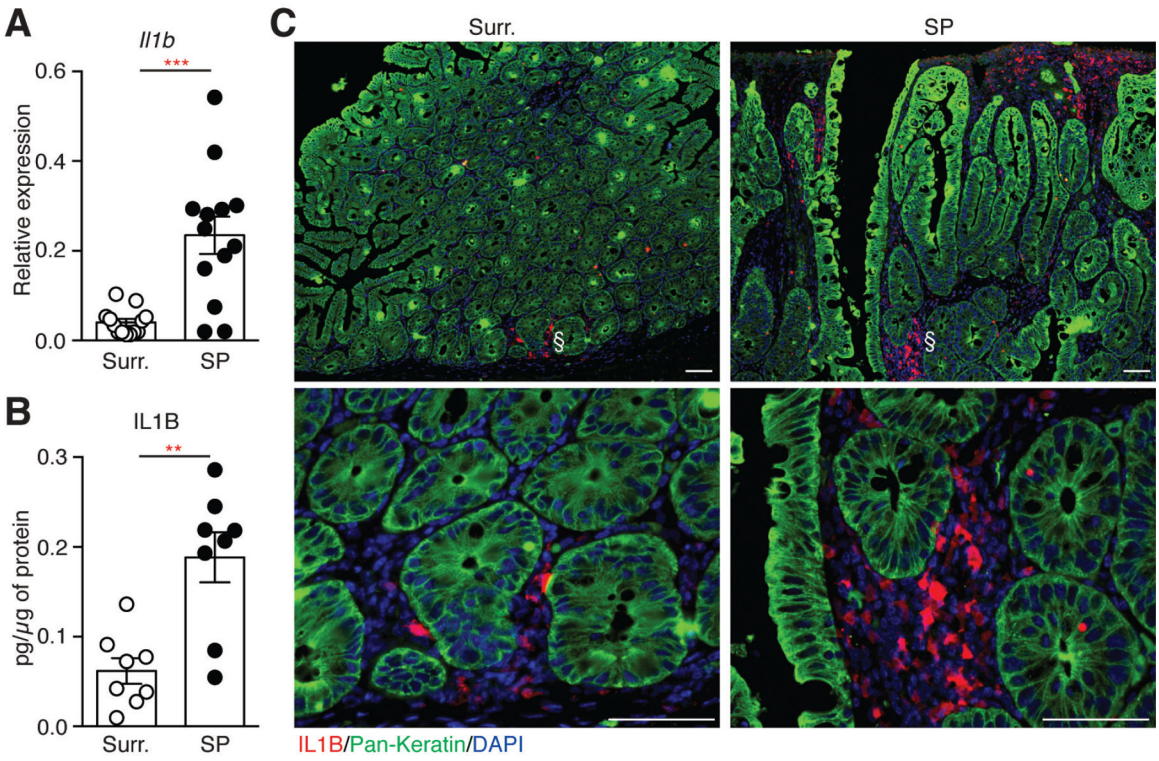


**Figure 2. IL1B expression is upregulated in SPs.**

(*A*) Il1b mRNA expression in tissue obtained from SPs compared with unaffected surrounding cecal tissue (n=13). (*B*) IL1B protein in tissue homogenates obtained from SPs compared with unaffected surrounding cecal tissue detected using ELISA (n=8). Data were normalized to μg of total protein extracted from SPs or unaffected surrounding cecal tissues. (*C*) Representative images of immunofluorescence stainings of IL1B (red) in surrounding tissues (left) and in SPs (right). Epithelial cells stained with anti-pan-keratin (green) and cell nuclei were counterstained with DAPI (blue). Bottom panels show a higher-magnification image of top panels. Representative images of three independent experiments are shown (n=7). $^{**}P < .01$, $^{***}P < .001$, by nonparametric Mann–Whitney test. Error bars indicate SEM. Scale bars,100 μm.

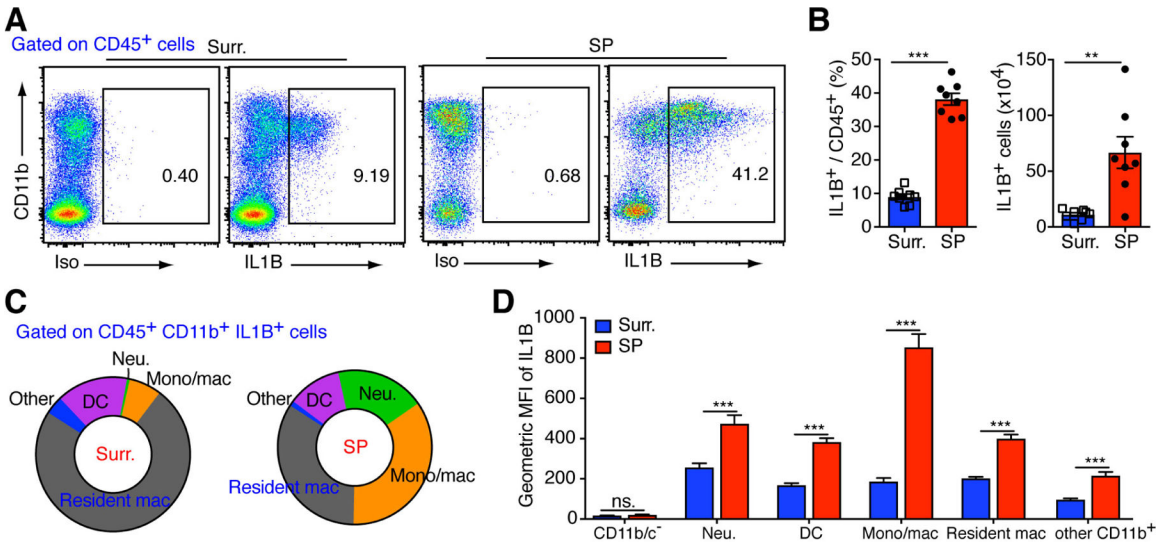


**Figure 3. IL1B is produced predominantly by inflammatory macrophages/monocytes in SPs.**

(*A*) Representative flow cytometry plots showing IL1B expression in $CD45^{+}CD11b^{+}$ population in SPs and surrounding tissues. (*B*) Relative (left) and absolute (right) number of IL1B producing cells in SPs and surrounding tissues. (*C*) Flow cytometric analysis of the of IL1B-producing cells in SPs and surrounding tissues. (*D*) IL1B mean fluorescence intensity (MFI) (bottom panels) from SPs compared with unaffected surrounding cecal tissues. Also see Supplementary Figure 6 for the gating strategy used for the identification and quantification of epithelial cells (Epcam+), SinglecF+ cells, neutrophils (Neu), DC, resident macrophage (mac) and inflammatory monocytes/ macrophages (Mono/mac). Ns, not significant, **P < .01, ***P < .001; by nonparametric Mann–Whitney test.

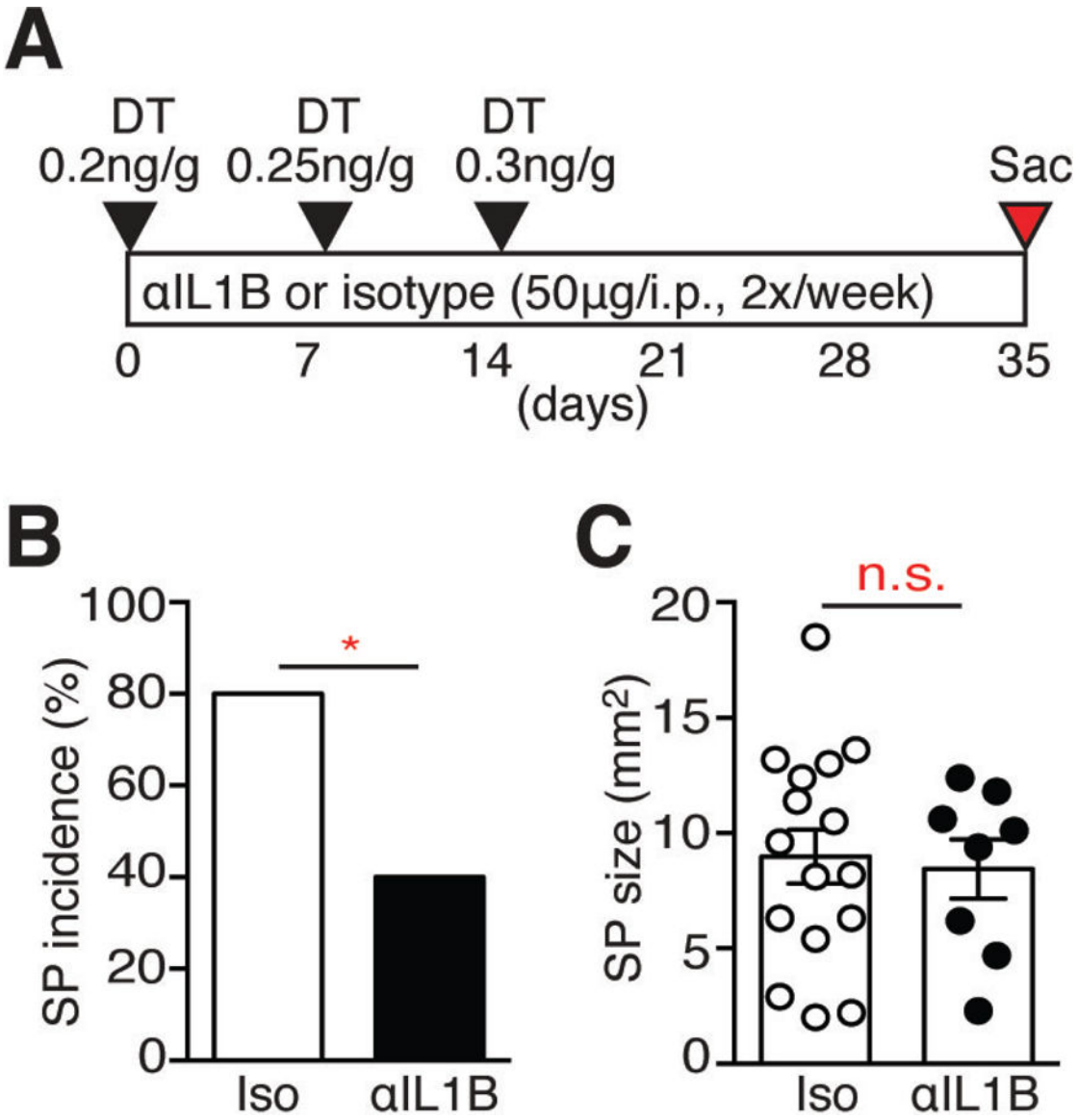


**Figure 4. IL1B neutralization reduces SP incidence.**

(*A*) Schematic representation of DT administration with anti-IL1B or isotype control treatment. (*B*) SP incidence in isotype-treated *HBUS* mice (80%, n=20, white bar) compared with *HBUS* mice treated with anti-IL1B(40%, n=20, black bar). **P* < .05, by Fisher's exact test. (*C*) SP size of isotype-treated *HBUS* mice (n=16) compared with anti-IL1B-treated *HBUS* mice (n=8). n.s. not significant, by nonparametric Mann–Whitney test. Error bars indicate SEM.

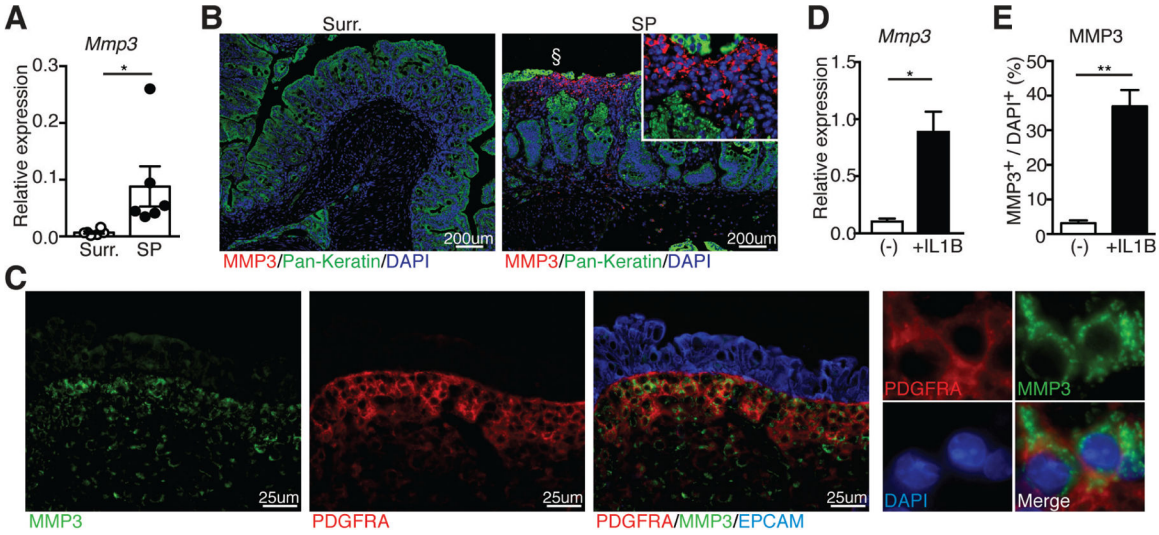


**Figure 5. PDGFRA$^+$ fibroblasts locate in the areas close to lumen of SPs and produce MMP3 *in vivo* and *in vitro* in response to IL1B stimulation.**

(*A*) *Mmp3* mRNA expression in tissue obtained from SPs compared with unaffected surrounding cecal tissue (n=6). (*B*) Representative images of immunofluorescence staining of MMP3 (red) in surrounding tissue (left) and in SPs (right). Epithelial cells stained with anti-pan-keratin (green) and cell nuclei were counterstained with DAPI (blue). Inset shows a higher-magnification image of §. Scale bars, 200 μm. (*C*) Representative images of immunofluorescence staining of MMP3 (green), PDGFRA (red) and epithelial cells (EPCAM+, blue) in SPs. Notice that co-staining of PDGFRA and MMP3 in SPs of the *HBUS* mice. Scale bars, 25 μm. (*D*) *Mmp3* mRNA expression in cultured PDGFRA$^+$ fibroblasts left unstimulated (white bar) or stimulated with recombinant IL1B for 6 hr (black bar) (n=3). (*E*) Percentage of cultured PDGFRA$^+$ fibroblasts express MMP3 protein (white bar, cells left unstimulated; black bar, cells stimulated with recombinant IL1B for 24 hr) (n=3). **P* < .05, ***P* < .01, by unpaired t-test. Error bars indicate SEM.

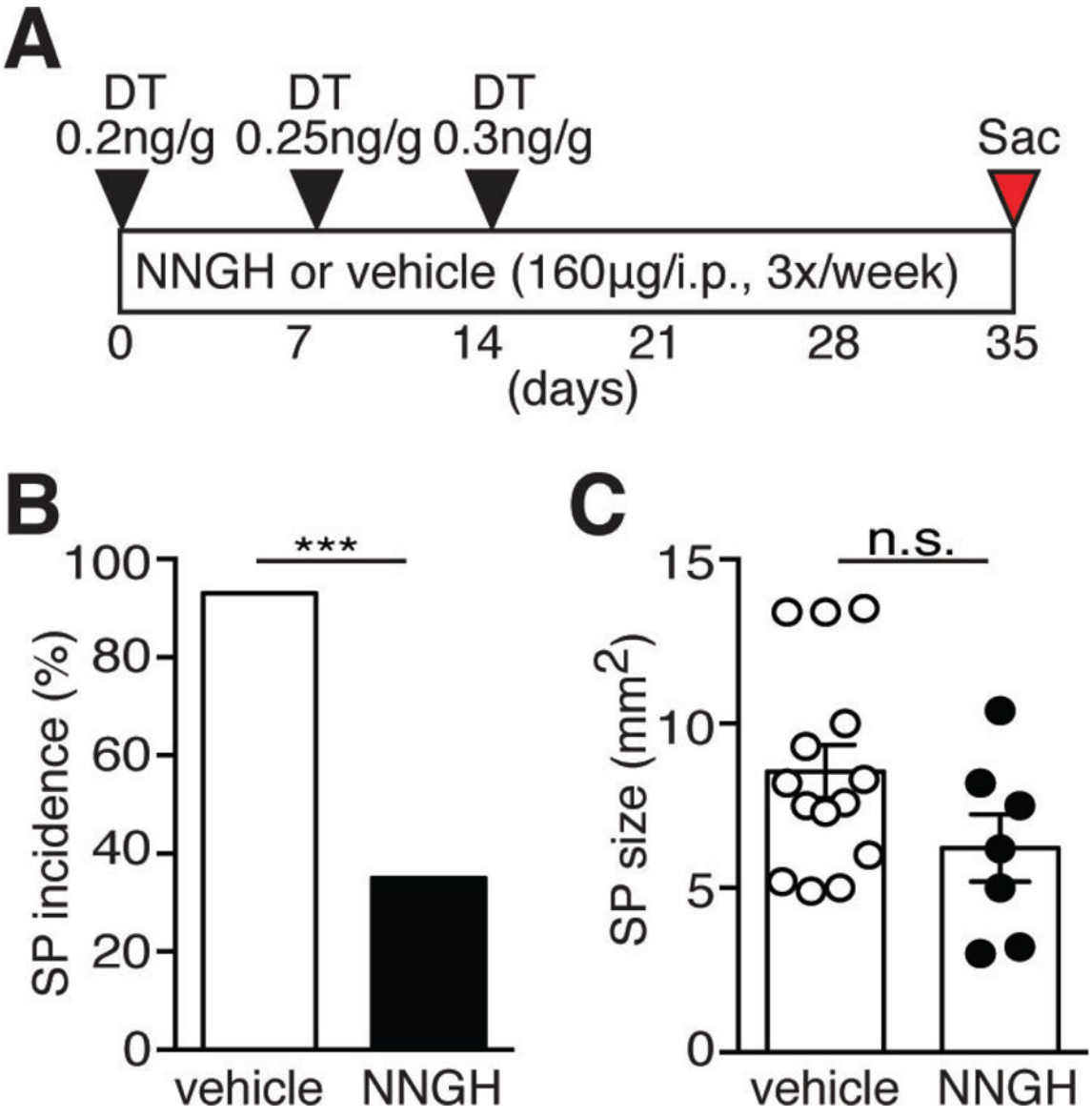


**Figure 6. MMP inhibition reduces SP incidence.**

(*A*) Schematic representation of DT administration with NNGH or vehicle treatment. (*B*) SP incidence in vehicle-treated *HBUS* mice (93%, n=15, white bar) compared with *HBUS* mice treated with NNGH (35%, n=20, black bar). ***$P < .001$, by Fisher's exact test. (*C*) SP size of vehicle-treated *HBUS* mice (n=14) compared with NNGH-treated *HBUS* mice (n=7). n.s. not significant by nonparametric Mann–Whitney test. Error bars indicate SEM.

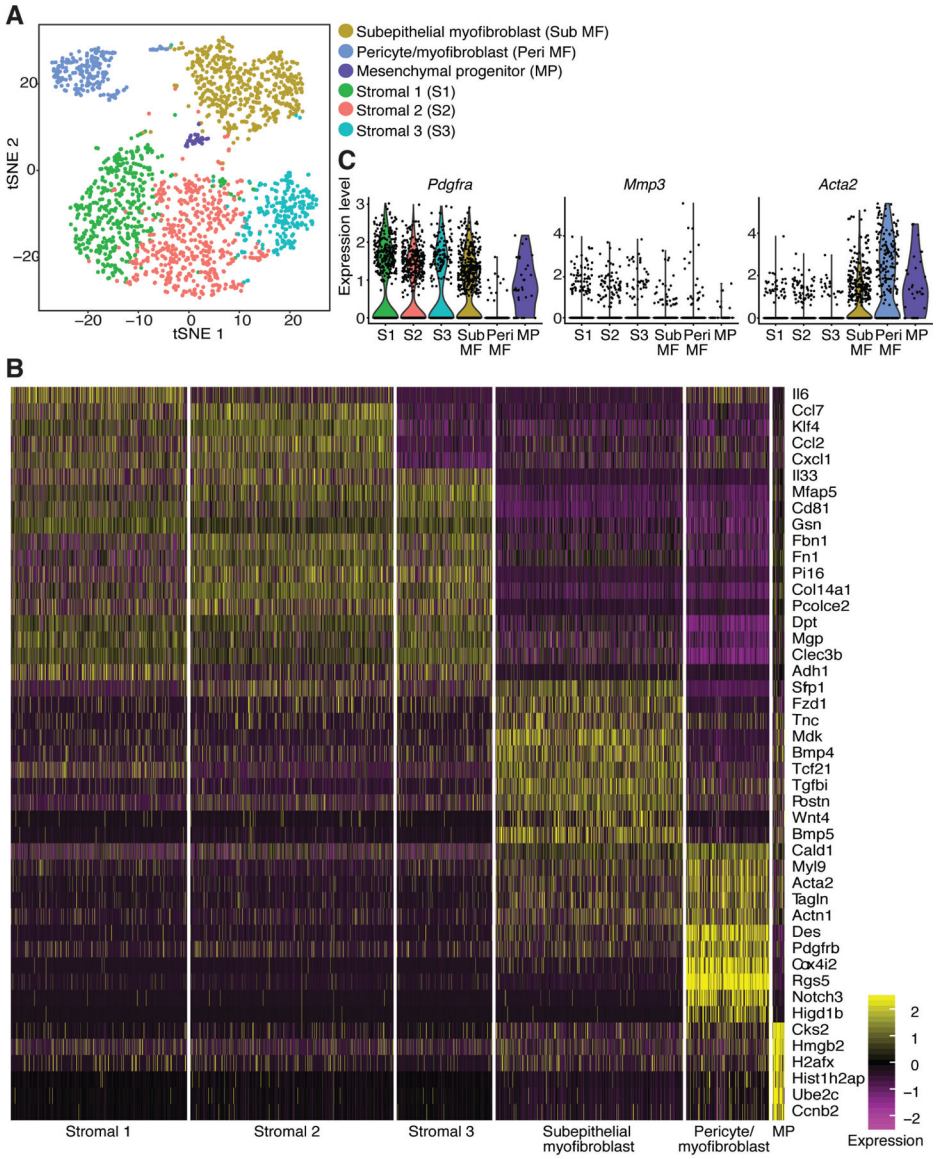


**Figure 7. Mesenchymal heterogeneity in SPs.**

(*A*) t-SNE plot of SP mesenchyme dataset. Single cells colored by cluster annotation. Descriptive cluster labels are shown. (*B*) Differential expression analysis of selected genes of SP-associated fibroblast clusters. (*C*) Violin plots for *pdgfra*, *mmp3* and *acta2*.